Morphology control of zinc oxide nanoparticles

Luís Filipe Marques Rodrigues, Prof. Dr. Carlos Miguel Calisto Baleizão[1]

[1] Supervisor, Instituto Superior Técnico, Universidade de Lisboa, Portugal

November 2022

Abstract: Zinc oxide is a metal oxide semiconductor that has aroused increasing interest in various fields of science due to its unique properties. The main objective of this work was to understand the growth mechanism of zinc oxide nanoparticles by the sol-gel method and how the synthesis parameters (pH, precursor concentration, solvent, reaction time and temperature) affect their final structure, namely their morphology and size. The results showed that the formation of ZnO is favoured due to the higher concentration of OH^- and the nanoparticles size decreased with increasing pH value, in basic medium. The nanoparticles diameter also increased with decreasing precursor concentration and they were larger when the solvent used was water, compared to methanol. The reaction times analysed did not change the nanoparticles, and the temperature experiments were inconclusive, there was no clear morphological change with the temperature variation. In all experiments, the nanoparticles are spherical and most particle sizes are between 5 and 13 nm. A second objective of this thesis was to develop mesoporous zinc oxide nanoparticles by the sol-gel method. Currently there are very few approaches to try to synthesize these particles and the existing ones still do not allow obtaining scalable and versatile syntheses, with well-defined morphologies, and controllable pore and particle sizes. To test the possibility of producing mesoporous zinc oxide nanoparticles, two sol-gel syntheses were performed, with one yielding mesoporous nanoparticles of about 107 nm. This method appears as a promising basis for a future development and optimization of mesoporous zinc oxide nanoparticles.

Keywords: Zinc Oxide; Nanoparticles; Mesoporous; Sol-gel synthesis.

1. Introduction

Zinc oxide (ZnO) is a metal oxide semiconductor that has aroused increasing interest from researchers in various fields of science. In nanotechnology, it has been extensively investigated due to its unique properties, such as relatively large exciton binding energy of about 60meV, direct wide band gap around 3.4eV, piezoelectricity, biocompatibility, or low manufacturing cost.[1] Such notable properties make it a very interesting material for a wide range of applications such as optoelectronic applications (e.g. LEDs, laser diodes, solar cells, transparent electrodes)[2,3], biomedical applications (e.g. anticancer / antibacterial applications, biosensing, drug-delivery, cosmetics)[4], environmental applications (e.g. gas sensor – detection of toxic and harmful gases, photocatalyst – degradation of organic pollutants)[5,6], or as industrial additive (paints, rubbers, adhesives).[7]

ZnO nanoparticles (NPs) can be synthetized from two different approaches: the top-down approach and the bottom-up approach. The top-down approach is based on physical methods that transform larger materials into smaller nano-sized particles. Despite allowing the production of nanoparticles on an industrial scale, it does not allow such rigorous control of the sizes of the particles and their uniformity. In opposition, through the bottom-up approach it is possible to chemically synthesize particles with the desired shape and size, in a very controlled way. [8]

Sol-gel is a bottom-up approach and one of the most versatile methods used to produce metal oxide nanoparticles. This method is very simple and cost effective, allows a great control of the size, porosity and morphology of the nanoparticles, it easily allows chemical doping and surface modification, and can be carried out at room temperature. For these reasons sol-gel is an efficient technique to produce high quality products, and thus it was the main used technique in this thesis.[9]

In this technique, a precursor is primarily hydrolysed, originating a colloidal solution (sol), which after polycondensation forms a gel-like

substance (gel). After aging, the gel is dried, and the final nanostructures are obtained. In some cases, it may be justified to apply a thermal treatment/calcination to the product obtained (Figure 1). [9]

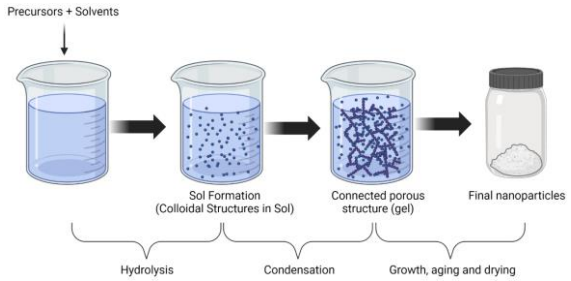

Figure 1 - Schematic representation of the sol-gel process. Created in BioRender, adapted from [9]

One of the most used zinc source precursors in the preparation of ZnO NPs is zinc acetate dihydrate. Sodium hydroxide is also one of the most reported hydrolysing agents and pH controllers for these syntheses. The chemical reactions involved in the formation of ZnO whose initial precursor is zinc acetate dihydrate $[Zn(CH_3COO)_2 \cdot 2H_2O]$ and in which is used sodium hydroxide $(NaOH)$ as a hydrolysing agent and pH controller, can be described by Equations 1 – 3:[10]

$$Zn(CH_3COO)_2 \cdot 2H_2O + 2NaOH \rightarrow Zn(OH)_2 + 2CH_3COONa + 2H_2O \quad (1)$$

$$Zn(OH)_2 + 2H_2O \rightarrow Zn(OH)_4^{2-} + 2H^+ \quad (2)$$

$$Zn(OH)_4^{2-} \rightarrow ZnO + H_2O + 2OH^- \quad (3)$$

The synthesis of zinc oxide nanoparticles is strongly affected by the external conditions such as pH of the solution, precursor concentration, reaction time and temperature or the solvent used. Therefore, the control of the synthesis parameters is essential to obtain the desired set of characteristics in the final nanoparticles. [10-12]

The aim of this work is to understand the growth mechanism of zinc oxide nanoparticles by sol-gel method, and how their synthesis parameters affect their final structure, namely their morphology and size. Although there are some articles on the influence of certain synthesis parameters on the characteristics of zinc oxide nanoparticles, their role is still not clear, and the information available is sometimes contradictory. A second objective of this work is to develop mesoporous zinc oxide nanoparticles (MZNs) by the sol-gel method. Zinc oxide is a material whose interest has been increasing in recent times and if it is possible to combine it into a mesoporous nanostructure, it could add value to currently existing mesoporous nanoparticles, due to its unique optical properties. It could also be of great interest for drug delivery applications for example. Currently there are no well-developed syntheses that allow obtaining stable mesoporous ZnO NPs with well-defined morphologies.[13-15] This work provides a starting point for the investigation of this specific type of particles and for the understanding of the growth mechanism of ZnO nanoparticles.

2. Experimental Part

2.1. Materials and Equipment

For the sol-gel syntheses of ZnO nanoparticles, the following materials were used: zinc acetate dihydrate ($[Zn(CH_3COO)_2 \cdot 2H_2O]$, ≥ 98%, Sigma-Aldrich) as zinc source, sodium hydroxide (pure NaOH, pellets, PanReac AppliChem) as hydrolysing agent and pH controller, and absolute methanol (MeOH, ≥99.9%, Riedel-de Haën), and deionized water (produced from a Millipore system Milli-Q ≥18 MΩcm with a Millipak membrane filter 0.22 µm) as solvents. Absolute ethanol (EtOH, ≥99.8%, Riedel-de Haën) was used as solvent in the solvothermal and mesoporous syntheses. It was also used to wash the particles and disperse them before the TEM images. For the synthesis of mesoporous nanoparticles an ammonium hydroxide solution (~25% NH_3 basis, Sigma-Aldrich) was also utilized and hexadecyltrimethylammonium bromide (CTAB, ≥99%, Sigma) was used as cationic surfactant.

The nanoparticles were centrifuged using a Sigma 2k15, with a 12141 rotor, at 19890 g and 20ºC. The polypropylene tubes used had a volume capacity of 10 mL. The centrifugations of the mesoporous nanoparticles were carried on a Beckman Coulter, model Avanti J30I at 30 000 and 80 000 g at 20ºC. The polypropylene tubes used had a volume capacity of 40 mL.

A Hitachi transmission electron microscope, model H-8100, equipped with a 200kw accelerator voltage and a LaB_6 filament was used to obtain the TEM images of the nanoparticles. The images were digitally acquired with a KeenView camera (Soft Imaging System) incorporated in the microscope. The samples for analysis were prepared by dispersing the nanoparticles in ethanol and dipping a copper grid coated with carbon in the dispersion, which was then left to air dry. The software ImageJ was used to analyse and estimate the size, shape factor (n) and morphology of the nanoparticles by evaluating at least 50 nanoparticles in each image.

The shape factor (n) corresponds to the ratio of the Feret diameter (farthest possible distance between the two parallel tangents of an object) with the minimum Feret diameter of the particle (closest possible distance between the two parallel tangents of an object) (Equation 4). This parameter allows the evaluation of the shape of the nanoparticles. The closest the shape factor is to 1, the more spherical are the particles. [16]

$$n = \frac{Feret\ Diameter}{Minimum\ Feret\ Diameter} \quad (4)$$

2.2. Sol-gel synthesis of ZnO NPs

Initially a control synthesis (*SG1*) was defined.

SG1 (control): ZnO sol was prepared by adding 1g of zinc acetate dihydrate under magnetic stirring into 23 mL of methanol (0.2M), at room temperature, until a clear solution was obtained (5 min proved to be enough). Then, a 5M sodium hydroxide solution (in methanol) was added drop-by-drop to adjust the pH value of the solution to 9. The resulting milky white gel was kept under stable stirring for another 2h and 30min. After that, the dispersion was centrifuged (19890 g, 15mins) and washed 3 times with absolute ethanol. In the last cycle, the supernatant was removed, and the nanoparticles were dried at 50 °C in a ventilated oven (*Figure 2*).

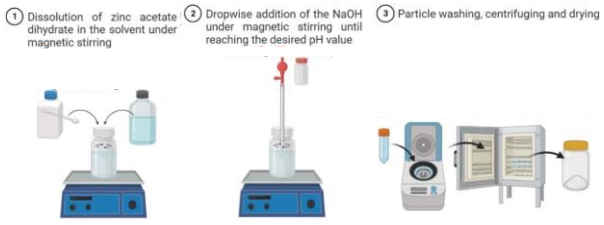

Figure 2 - Schematic representation of sol-gel synthesis of ZnO NPs. Created with BioRender.

Subsequent changes were made to the synthesis parameters in order to understand their influence on the characteristics of the final particles. In *SG2* and *SG3* the pH values of the solutions were changed to 7 and 11, respectively. In *SG4* and *SG5* the initial precursor concentration was changed to one-third and two-thirds of the control experiment value. In *SG6* the solvent used was water. *SG7* and *SG8* introduce variations in reaction time to 30min and 1h, respectively. Finally, in *SG9* and *SG10* the reactions were carried out at 40 and 60ºC, respectively. The syntheses carried out are summarized in Table 1.

Table 1 - Experiments and corresponding synthesis parameters

Exp.	pH	T (ºC)	Precursor concentration (M)	Solvent	time (h)
SG1	9	RT	0.2	MeOH	2.5
SG2	7	RT	0.2	MeOH	2.5
SG3	11	RT	0.2	MeOH	2.5
SG4	9	RT	0.07	MeOH	2.5
SG5	9	RT	0.13	MeOH	2.5
SG6	9	RT	0.07	H_2O	2.5
SG7	9	RT	0.2	MeOH	0.5
SG8	9	RT	0.2	MeOH	1
SG9	9	40	0.2	MeOH	2.5
SG10	9	60	0.2	MeOH	2.5

2.3. Solvothermal synthesis of ZnO NPs

The solvothermal synthesis (henceforth referred to as *ST* experiment) was carried out as described by Achouri et al.[17] In a polypropylene bottle 511 mg of zinc acetate dihydrate were dissolved in 35 mL of ethanol under magnetic stirring. A NaOH solution (96 mg NaOH in 35 mL ethanol) was added dropwise and the mixture was stirred at room temperature for 30 min. Then, the solution was transferred into a 140 mL Teflon-sealed autoclave and was heated at 160 °C for 24h. After cooling, the dispersion was centrifuged (19890 g, 15mins), washed 3 times with water, one with absolute ethanol, and dried at 70 °C overnight, as represented by Figure 3.

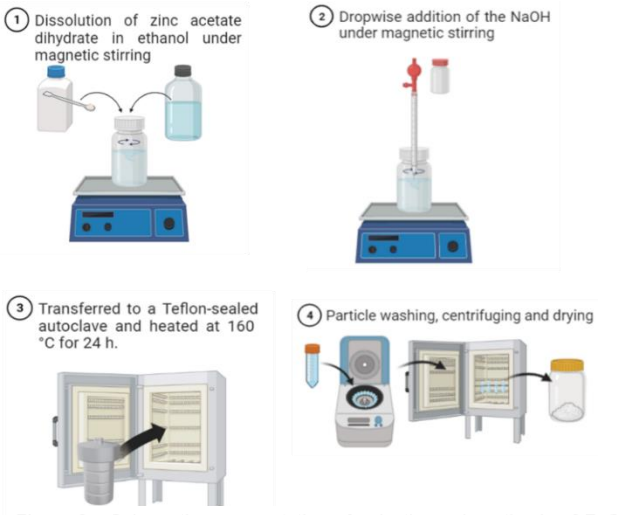

Figure 3 - Schematic representation of solvothermal synthesis of ZnO NPs. Created with BioRender.

2.4. Syntheses of MZNs

Two main syntheses were carried out: *Meso1* and *Meso2*.

Meso 1: *Meso1* was adapted from the work described by Ribeiro et al.[18] First, 0,5 g of CTAB were dissolved in 230 mL of water at 32ºC, under stable magnetic stirring. After the temperature has stabilized, 1,75 mL of a 1.5M NaOH solution (in water) was added. After 30 min, 10 mL of an as prepared 1.1M zinc acetate dihydrate solution (in water) was carefully added dropwise to the solution. The reaction proceeded for 3 h and then the dispersion was centrifuged (80000 g, 15mins) and washed 2 times with distilled water and 2 times with absolute ethanol. In the last cycle, the supernatant was removed, and the nanoparticles were dried at 50 °C in a ventilated oven.

Meso2: *Meso2* was adapted from the work described by Rodrigues et al.[19] Initially 0,113 g of CTAB were dissolved in 58,7 mL of an as prepared 0.5M ammonium hydroxide solution (in water) at 50ºC, under stable magnetic stirring. After 30 min, 12,2 mL of a 0.15M zinc acetate dihydrate solution (in ethanol) was added dropwise to the solution. The reaction proceeded for 6 h and then the solution was left to age in a ventilated oven at 50ºC for 24h. After cooling, the dispersion was centrifuged (30000 G, 20 minutes) and washed 2 times with a mixture of 1:1 water/ethanol and 3 times with only absolute ethanol. In the last cycle, the supernatant was removed, and the nanoparticles dried at 50 °C in a ventilated oven.

3. Results and discussion

3.1. Sol-gel syntheses and characterization of ZnO NPs

SG1 was defined as the control synthesis and was performed at pH=9, during 2h30, at room temperature, with an initial precursor concentration of 0.2M and methanol as solvent. Syntheses *SG2-SG10* have the same base procedure as *SG1*, with a synthesis parameter being varied to analyse its influence on the final nanoparticles.

The average diameter of the ZnO NPs obtained for *SG1* was 8 ± 1 nm with an average shape factor of 1,2 ± 0,2. The *SG1* procedure was repeated and proved to be reproducible (Table 2). Both syntheses presented particles with very similar sizes and almost spherical. Figure 4 shows the TEM image and diameter distribution analysis of *SG1*.

Table 2 - Results from SG1 and its repetition

Experiment	Particle diameter (nm)	Shape factor
SG1 (control)	8 ± 1	1,2 ± 0,2
SG1 (repetition)	9 ± 1	1,1 ± 0,1

The reaction yield obtained for this synthesis was about 88%. In all experiments, the reaction yield was determined through the ratio between the obtained mass of ZnO and the expected mass of ZnO. The expected mass of ZnO was calculated assuming that the number of moles of the initial zinc precursor is equal to the number of moles of ZnO (Equations 1-3).

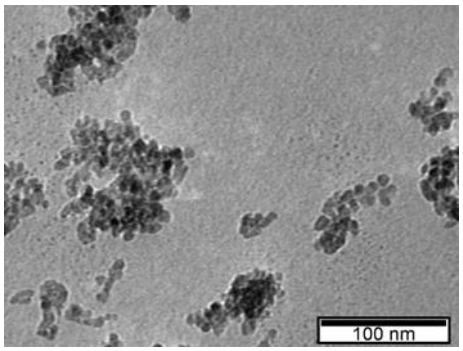

Figure 3 - TEM image of ZnO NPs synthesized by SG1

3.1.1. Influence of the pH in the particle size

In order to understand the pH effect on the size of the final nanoparticles, the pH value of the solution was changed while the remaining conditions were kept constant (precursor concentration, solvent, reaction time and temperature). *SG2* and *SG3* tested pH values of 7 and 11 respectively.

In *SG2* it was not possible to obtain particles during the centrifugation stage, and therefore no TEM images were taken. In the control synthesis, when NaOH is added to the solution, the resulting mixture becomes opaque and takes on a milky white tone. This phenomenon was not observed in this case, indicating that the particles did not form. These results seem to confirm that when the concentration of OH^- ions is lower, it becomes more difficult to form the growth unit $Zn(OH)_4^{2-}$ and consequently to obtain ZnO particles. *SG3* proceeded normally and the corresponding TEM images are shown in Figure 5.

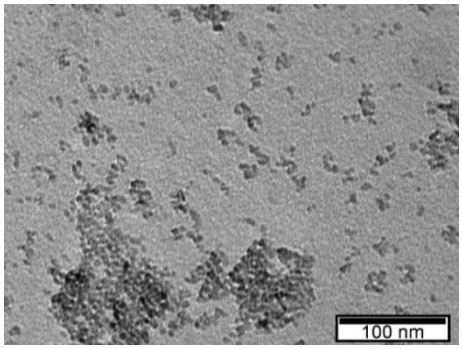

Figure 4 - TEM image of ZnO NPs synthesized at pH 11

The average diameter of the ZnO NPs obtained was 5 ± 1 nm, the average shape factor was 1,1 ± 0,1 and the reaction yield was 51%. Comparing this result with the control experiment (pH=9) it is possible to observe a decrease in yield and in the size of the nanoparticles with the increase of the pH value, in alkaline medium. This result is also in agreement with the literature.[10][20] In basic media, the formation of zinc oxide is favoured due to the decisive role of OH^- in the formation of the growth unit $Zn(OH)_4^{2-}$ (Equations 1 - 3). An increase in the pH value leads to an increase in nucleation and growth rates. This phenomenon affects the final size of the particles, as the results show, as more nuclei are formed. The same amount of material is distributed over more growing particles, resulting in smaller size nanoparticles. However, the reaction yield value significantly decreased from pH 9 to pH 11. This may be related to the dissolution effect of zinc oxide nanoparticles at higher pH values (Equation 3 – inverse reaction).[10] This could be a possible explanation for the decrease in the reaction yield and, if so, this dissolution will also contribute to the decrease in the size of the final nanoparticles. In this way, the results show that, of the tested pH values, pH = 9 is the one that presents the best conditions, because it presents the highest yield and possibly is the value at which the particles are most stable. The shape of the particles does not change significantly with the change in pH value.

3.1.2. Influence of the precursor concentration

The initial precursor concentration was also varied to understand its effect on the final nanoparticles. Its value was changed to one third (*SG4*) and two thirds (*SG5*) of the control experiment, while the remaining conditions were kept constant (pH, solvent, reaction time and temperature). Figure 6 shows the TEM images for the *SG4* and *SG5* syntheses, as well as the corresponding diameter distribution analyses.

The average diameter of the ZnO NPs obtained was 13 ± 3 nm and 8 ± 1 nm for *SG4* and *SG5*, respectively, with average shape factors of 1,2 ± 0,1 and 1,2 ± 0,1. The corresponding reaction yield values are 98% and 49%.

The nucleation rate equation can help clarify these results. The nucleation rate, J_N , can be expressed in terms of critical free energy, ΔG_{crit}, and a pre-factor, J_0 :[21]

$$J_N = J_0 \exp\left(-\frac{\Delta G_{crit}}{k_B T}\right) = J_0 \exp\left(\frac{-16\pi v^2 \gamma^3}{3(k_B T)^3 (\ln S)^2}\right) \quad (5)$$

where T is the temperature, k_B the Boltzmann's constant, S the supersaturation of the solution, given by c_1/c_s , with $c_1$the precursor concentration and c_s the solubility of the solid phase, γ the surface energy, and v the molar volume.

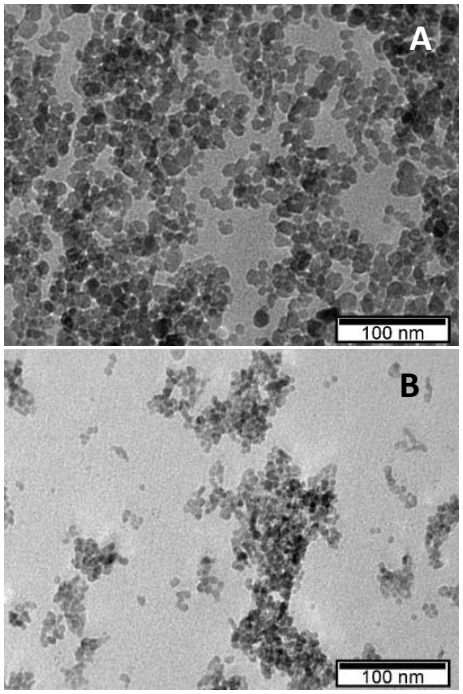

Figure 6 – A) TEM image of ZnO NPs synthesized with a precursor concentration of 0.07M; B) TEM image of ZnO NPs synthesized with a precursor concentration of 0.13M

According to the nucleation rate equation (Equation 5), the nucleation rate is expected to increase with increasing supersaturation, which is directly related with the precursor concentration. Fewer nuclei make bigger particles. Although the particle sizes did not vary from *SG1* to *SG5*, there was a clear increase in this parameter when observing *SG4* results. A broader interpretation of these results supports the expected growth behaviour, that particle size increases with

decreasing concentration of the initial precursor. Despite the variation in particle sizes, the shape factor remained unchanged in the three experiments. Regarding the reaction yields, *SG4* approaches a value of 100%, while in *SG5* there was a decrease to approximately half of that value. Due to the high difference in these values and the lack of a clear pattern for evaluating them, no conclusion is drawn regarding this.

3.1.3. Influence of the synthesis solvent

The main objective of *SG6* was to test the use of a non-alcoholic solvent, more specifically water, and to understand its effect on the final nanoparticles. This synthesis was performed with one third of the precursor concentration of the control experiment, and as such, *SG4* is the experiment that serves as a comparison to *SG6* results, as they present the same amount of initial precursor. TEM images were taken (Figure 7).

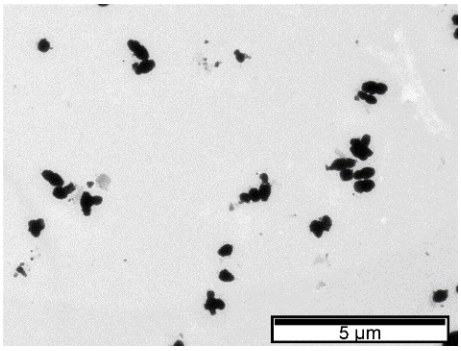

Figure 7 –TEM image of ZnO NPs synthesized by solvothermal method

The average diameter of the ZnO NPs obtained was 370 ± 119 nm, the average shape factor was 1,3 ± 0,2 nm and the reaction yield was 85%. An interpretation of these results must be made considering the values of dielectric constant and polarity of methanol and water, presented in Table3.

Table 3 -Solvent properties

Solvent	Relative polarity[22]	Dielectric constant [23]
Methanol	0,762	32
Water	1	80

A possible explanation for this large difference in the size results may be related to the electrostatic repulsive energy values. The electrostatic repulsive interaction energy is directly proportional to the polarity and inversely proportional to the dielectric constant of the solvent molecules.[12] Among the two solvents, water possess the highest polarity, which in a first analysis would translate into an increase in repulsive interaction. However, at the same time, the dielectric constant of water appears to be large enough to reduce this repulsion, and to produce larger particles than the synthesis carried out in methanol. Regarding the reaction yields, *SG4* is not the best experiment for comparisons since there is no complete confidence in this result. However, the *ST* value is similar to that of *SG1* and is greater than 80%, so there are no large variations in the reaction yield that would allow one method to be preferred over another.

3.1.4. Influence of the reaction time

In *SG7* and *SG8*, the effect of the reaction time on the final nanoparticles was studied. Its value was changed from 0.5h (*SG7*) to 1h (*SG8*), while the remaining conditions were kept constant (pH, precursor concentration, solvent, and temperature). Figure 8 shows TEM images of the respective obtained nanoparticles.

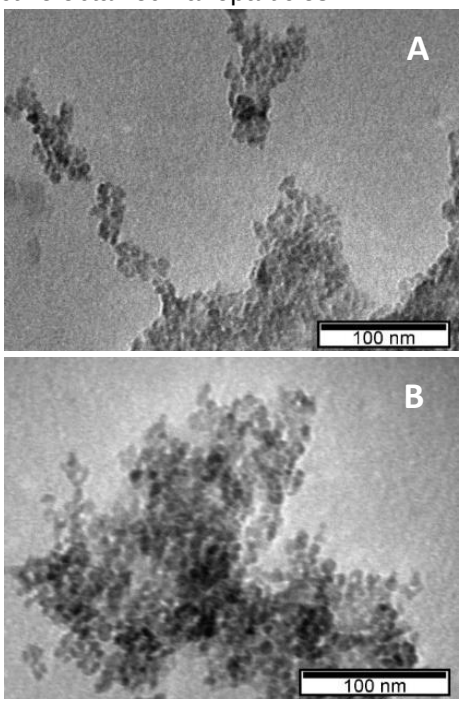

Figure 8 –A) TEM image of ZnO NPs synthesized in 0.5h; B) TEM image of ZnO NPs synthesized in 1h

The average diameter of the obtained ZnO NPs was 8 ± 2 nm for both and average shape factors of 1,2 ± 0,1 and 1,1 ± 0,2 (*SG7* and *SG8*, respectively). The corresponding reaction yield values were 77% and 80%.

The results show that there was no change in the size of the nanoparticles and in the shape factor with the variation of the reaction time. This may indicate that in the first 0.5h of reaction, the

particles are already formed and well established, so that the additional reaction time will not significantly affect the size of the nanoparticles. However, the reaction yield, which is an important factor to have into account, increased by 11% from 0.5h to 2.5h, suggesting that an increase in the reaction time will favour an increase in the reaction yield. This variation is significant and as such, for each case, a discussion should be made about which parameter is most valued, the time spent in the synthesis, or the amount of final product obtained.

After nucleation and growth, it is expected that the average particle size continues to increase with time due to coarsening mechanisms.[22] In this case, this relationship was not verified, which may indicate that the coarsening mechanisms are not present, or that they would require much more time to be noticed.

3.1.5. Influence of the reaction temperature

In order to understand the effect of the reaction temperature on the final nanoparticles, its value was changed while the remaining conditions were kept constant (pH, precursor concentration, solvent and reaction time). Figure 9 shows TEM images of *SG9* (40ºC) and *SG10* (60ºC).

The average diameter of the obtained ZnO NPs was 10 ± 2 nm and 7 ± 2 nm for *SG9* and *SG10*, respectively, with average shape factors of 1,3 ± 0,2 and 1,2 ± 0,2. The corresponding reaction yield values were 55% and 73%.

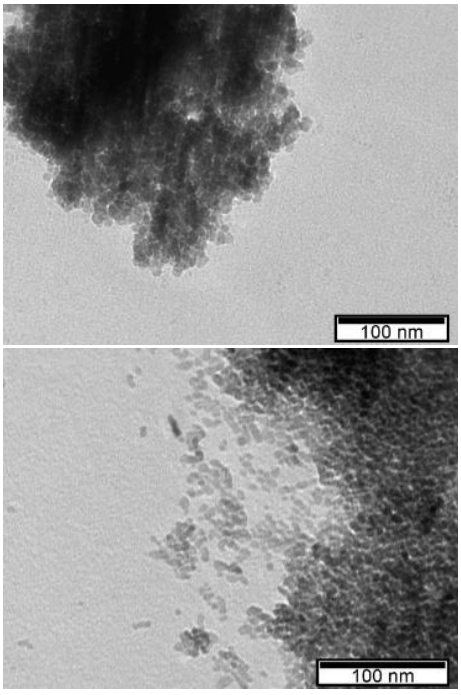

Figure 9 –A) TEM image of ZnO NPs synthesized at 40ºC; B) TEM image of ZnO NPs synthesized at 60ºC

Several synthesis parameters are temperature dependent. For higher temperatures, the nucleation rate decreases (Equation 5), which results in bigger final particles since the same amount of matter is distributed over less nuclei. Surface energy or solvent viscosity are other examples of factors that are influenced by temperature. The higher the temperature, the lower the surface energy and the lower the viscosity.

Analysing the coarsening rate constant, given by:[22]

$$k = \frac{8\gamma v^2 c_{r=\infty}}{54\pi\eta a N_A} \quad (6)$$

where $c_{r=\infty}$ is the equilibrium concentration at a flat surface, η is the viscosity of the solvent, N_A the Avogadro's number, and a is the solvated ion radius, it is possible to notice that a decrease in surface energy contributes to decrease this constant, but a decrease in viscosity tends to increase it (here the temperature contributes simultaneously, but in different ways, to the increase and decrease of particle sizes by coarsening mechanisms). Since the reaction time results did not reveal the presence of coarsening mechanisms and changes in the particle size by these aging processes, it is possible that the aforementioned temperature effects also do not influence the size of the particles obtained.

The obtained results did not show a clear change in the particle size with the temperature variation and, as such, no conclusion should be drawn from this analysis. Regarding the particles morphology analysis, their shape is approximately spherical for the three experiments, with no alterations in the shape factor. Regarding the reaction yield values, the results were also not very clear. This parameter decreased 33% from room temperature to 40ºC and increased 18% from 40ºC to 60ºC. Once again, it was not verified a clear and logic variation and as such, no conclusions should be drawn from here.

3.2. Solvothermal synthesis and characterization of ZnO NPs

In order to compare the results obtained by sol-gel with other published methods to synthesize ZnO NPs, a solvothermal synthesis was performed, as described by Achouri et al.[17].The ZnO NPs were analysed by TEM imaging (Figure 10).

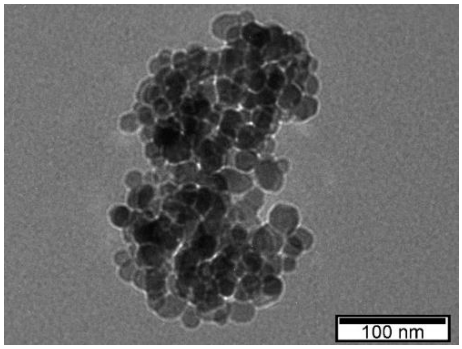

Figure 10 –TEM image of ZnO NPs synthesized by solvothermal method

The obtained nanoparticles have an average particle diameter of 25 ± 11 nm and an average shape factor of 1,2 ± 0,1. The reaction yield was about 65%.

There are some differences in the synthesis parameters comparing the solvothermal experiment and the control experiment. Even so, the ones that have the greatest impact, as they present the greatest variation when compared, are the high temperature, high pressure and high reaction time. This reaction proceeded at 160°C for 24h in a Teflon-sealed autoclave.

The results show that the particle size obtained is larger than any of the previous (except the synthesis in water). Analysing the results, this solvothermal synthesis does not seem to bring morphological and size advantages when compared with the sol-gel syntheses. The increase in size may be an advantage or disadvantage, depending on the intended application, however the respective standard deviation is relatively high, the highest observed, indicating that the particles have more heterogeneous sizes. The morphology of the particles does not seem to have undergone great variation, presenting an approximately spherical shape. The reaction yield in this case is lower than most sol-gel experiments tested.

In the solvothermal method, by increasing temperature and pressure, the fundamental properties (e.g. viscosity, density, dielectric constant, etc) of the solvent change. As temperature increases, the dielectric constant decreases and the ionic species can precipitate, leading to the formation of the ZnO nanoparticles. However, the mechanisms controlling the reactions are more difficult to verify when compared with the sol-gel method.

Therefore, focusing only on the results obtained regarding the size and morphology of the nanoparticles, it does not seem that the solvothermal synthesis presents significant advantages over the sol-gel synthesis, unless one wants to obtain particles with larger sizes. Sol-gel is a simpler method than solvothermal, in which the evolution of particle growth can be more easily analyzed and can be carried out at room temperature.

3.3. ZnO mesoporous nanoparticles

One of the main objectives of this thesis was to test the possibility of producing mesoporous zinc oxide nanoparticles. For this purpose, two sol-gel syntheses were tested: *Meso1* and *Meso2*. Both correspond to adaptations of MSN syntheses however with the use of zinc precursors to obtain zinc oxide nanoparticles. *Meso1* was adapted from the experiment described by Ribeiro et al.[18] and *Meso2* from the synthesis performed by Rodrigues et al.[19] *Meso1* was performed in water at 32ºC, with a NaOH solution as the base and *Meso2* was performed in water and ethanol, at 50ºC, with an ammonium hydroxide solution serving as the base. This was the starting point for trying to understand the mechanisms that could eventually originate this specific type of particles. For both cases, the nanoparticles were analysed by TEM imaging (Figure 11 - *Meso1*, Figure 12 - *Meso2*).

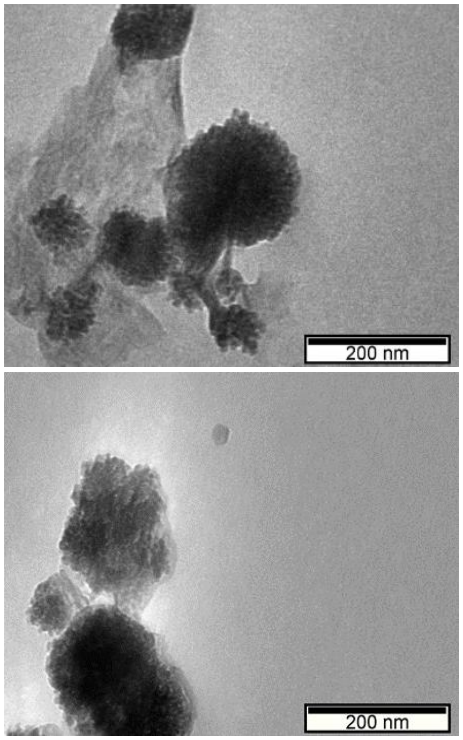

Figure 11 –TEM image of MZNs synthesized by the Meso1 synthesis

The TEM images *Meso1* suggest the existence of mesoporous zinc oxide nanoparticles (MZNs) with an average diameter of 107± 39 nm, an

average shape factor of 1.2 ± 0.1, and reaction yield of about 10%.

The formation of the expected mesoporous nanostructures, i.e. spherical nanoparticles with mesopores, is based on the use of a template, formed by the supramicellar assembly of cylindrical micelles. Once the zinc precursor is added, the hydrolysis/condensation reactions lead to the formation of zinc oxide around the micelles. The structural equilibrium of the supramicellar assembly is very susceptible to changes in the reaction system and if the ideal conditions are not obtained, the subsequent formation of these mesoporous particles is compromised. However, analyzing the obtained results, the growth of zinc oxide around micellar structures appears to have occurred.

Despite the relatively high standard deviation obtained, these results constitute a first base for the study of the formation of mesoporous zinc oxide nanostructures. More future studies will be necessary in order to verify the stability of these structures and to readjust the synthesis parameters to improve these results, especially the reaction yield which is very low.

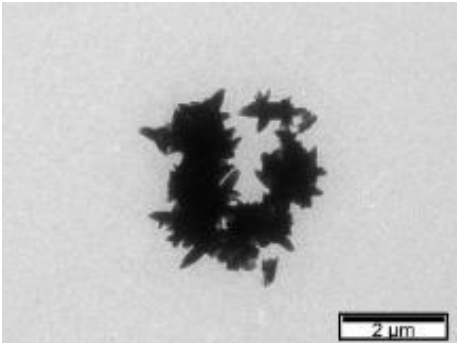

Figure 12 –TEM image of structures obtained by the Meso2

The *Meso2* TEM images reveal structures composed of rod-shaped nanoparticles. Due to the difficulty in evaluating the individual dimensions and morphology of these nanoparticles, the corresponding measurements were not performed. However, it is possible to observe from the scale of the Figure 12 that these particles and aggregates are much larger than any other obtained within the scope of this thesis. The reaction yield was estimated to be around 23%, again a very low value.

These results are quite different from what was expected and from *Meso1*. It is not possible to compare the two syntheses since several synthesis parameters vary. The main conclusion that can be drawn from these results is that this synthesis is not suitable for producing mesoporous zinc oxide nanoparticles.

4. Conclusions

With this work, we intended to understand the growth mechanism of zinc oxide nanoparticles by the sol-gel method in order to control their morphology. Initially, the influence of the synthesis parameters (pH, precursor concentration, solvent, reaction time and temperature) on the final zinc oxide nanoparticles was studied. Then a comparison of sol-gel synthesis with solvothermal synthesis was made. Finally, two attempts were made to produce mesoporous zinc oxide nanoparticles. The analysis of the results considered the diameters, morphology, and size distribution of the nanoparticles.

The syntheses carried out at different pH values (7, 9 and 11) allow us to conclude that in a basic medium, the formation of zinc oxide is favoured due to the higher concentration of OH- ions, which play a fundamental role in the formation of the growth unit $Zn(OH)_4^{2-}$. In neutral medium, the concentration of these ions is lower, so there was an inability to form particles. In basic medium, it was found that the higher the pH value, the smaller the particle size. For higher pH values, the reaction yield value significantly decreases, possibly due to the dissolution of the nanoparticles. For the experiments tested, the pH value with the most promising results was pH=9. The analysis of the initial concentration of zinc precursor (0.07, 0.13 and 0.20 M) revealed that the size of the particles increases with decreasing precursor concentration. The experiments in which the solvent was studied (methanol and water) revealed that the synthesis carried out in water resulted in particles with diameters about 50 times larger than those in methanol, and with a much more heterogeneous size distribution. Some solvent properties, such as polarity or dielectric constant, seem to have a decisive role in the characteristics of the obtained nanoparticles. The reaction times analysed (0.5, 1 and 2.5 h) did not change the final nanoparticles, however an increase in the reaction time suggests an increase in the reaction yield. The temperature experiments (room temperature, 40ºC, 60ºC) were inconclusive since there was not a clear change behaviour of the particle size with the temperature variation. In all experiments, the nanoparticles showed an approximately spherical morphology.

The solvothermal synthesis performed did not present comparative advantages over the sol-gel method considering the parameters evaluated. Larger particles with a more heterogeneous size

distribution were obtained and the reaction yield was lower for this method, when compared with sol-gel. The greater energy and time consumption of this synthesis and the lesser simplicity of the process compared to sol-gel justifies the use of the sol-gel method to produce ZnO NPs.

Of the mesoporous syntheses tested, the one that showed the most promising results was Meso1. It was possible to obtain mesoporous zinc oxide nanoparticles and, although the size distribution is broad, and the reaction yield is very low, it seems to be an excellent starting point for the future development and improvement of mesoporous zinc oxide nanoparticles.

5. References

[1] Klingshirn, C., Hauschild, R., Priller, H.,Decker, M., Zeller, J., & Kalt, H. ZnO rediscovered—once again!?. *Superlattices and Microstructures* **2005**, *38*(4-6), 209-222.

[2] Wibowo, A., Marsudi, M. A., Amal, M. I., Ananda, M. B., Stephanie, R., Ardy, H., & Diguna, L. J. ZnO nanostructured materials for emerging solar cell applications. *RSC advances* **2020**, *10*(70), 42838-42859.

[3] Djurišić, A. B., Ng, A. M. C., & Chen, X. Y. ZnO nanostructures for optoelectronics: Material properties and device applications. *Progress in quantum electronics* **2010**, *34*(4), 191-259.

[4] Mishra, P. K., Mishra, H., Ekielski, A., Talegaonkar, S., & Vaidya, B. Zinc oxide nanoparticles: a promising nanomaterial for biomedical applications. *Drug discovery today* **2017**, *22*(12), 1825-1834.

[5] Kang, Y., Yu, F., Zhang, L., Wang, W., Chen, L., & Li, Y. Review of ZnO-based nanomaterials in gas sensors. *Solid State Ionics* **2021**, *360*, 115544.

[6] Ong, C. B., Ng, L. Y., & Mohammad, A. W. A review of ZnO nanoparticles as solar photocatalysts: Synthesis, mechanisms and applications. *Renewable and Sustainable Energy Reviews* **2018**, *81*, 536-551.

[7] Sabir, S., Arshad, M., & Chaudhari, S. K. Zinc oxide nanoparticles for revolutionizing agriculture: synthesis and applications. *The Scientific World Journal*, **2014**

[8] Singh, T. A., Das, J., & Sil, P. C. Zinc oxide nanoparticles: A comprehensive review on its synthesis, anticancer and drug delivery applications as well as health risks. *Advances in Colloid and Interface Science* **2020**, *286*, 102317.

[9] Parashar, M., Shukla, V. K., & Singh, R. Metal oxides nanoparticles via sol–gel method: a review on synthesis, characterization and applications. *Journal of Materials Science: Materials in Electronics* **2020**, *31*(5), 3729-3749.

[10] Alias, S. S., Ismail, A. B., & Mohamad, A. A. Effect of pH on ZnO nanoparticle properties synthesized by sol–gel centrifugation. *Journal of Alloys and Compounds* **2010**, *499*(2), 231-237.

[11] Oskam, G., & Poot, F. D. J. P. Synthesis of ZnO and TiO2 nanoparticles. *Journal of sol-gel science and technology* **2006**, *37*(3), 157-160.

[12] Ramya, M., Nideep, T. K., Nampoori, V. P. N., & Kailasnath, M. Solvent assisted evolution and growth mechanism of zero to three dimensional ZnO nanostructures for dye sensitized solar cell applications. *Scientific reports* **2021**, *11*(1), 1-14.

[13] Lu, X., Zhang, H., Ni, Y., Zhang, Q., & Chen, J. Porous nanosheet-based ZnO microspheres for the construction of direct electrochemical biosensors. *Biosensors and bioelectronics* **2008**, *24*(1), 93-98.

[14] Bakrudeen, H. B., Sugunalakshmi, M., & Reddy, B. S. Auto-fluorescent mesoporous ZnO nanospheres for drug delivery carrier application. *Materials Science and Engineering: C* **2015**, *56*, 335-340.

[15] Barick, K. C., Nigam, S., & Bahadur, D. Nanoscale assembly of mesoporous ZnO: A potential drug carrier, *Journal of Materials Chemistry* **2010**, *20*(31), 6446-6452.

[16] Rosa, P. A. S. *Glutathione-Responsive Breakable Nanoparticles for Controlled Doxorubicin Release*, [Master's Thesis, Instituto Superior Técnico], **2021**.

[17] Achouri, F., Corbel, S., Balan, L., Mozet, K., Girot, E., Medjahdi, G., & Schneider, R. Porous Mn-doped ZnO nanoparticles for enhanced solar and visible light photocatalysis. *Materials & Design* **2016**, *101*, 309-316.

[18] Ribeiro, T., Rodrigues, A. S., Calderon, S., Fidalgo, A., Gonçalves, J. L., André, V., Duarte, M.T., Ferreira, P.J., Farinha, J. P. S., Baleizão, C. Silica nanocarriers with user-defined precise diameters by controlled template self-assembly. *Journal of colloid and interface science* **2020**, 561, 609-619.

[19] Rodrigues, A. S., Ribeiro, T., Fernandes, F., Farinha, J. P. S., & Baleizão, C. Intrinsically fluorescent silica nanocontainers: A promising theranostic platform. *Microscopy and Microanalysis* **2013**, 19(5), 1216-1221.

[20] Li, W. J., Shi, E. W., & Fukuda, T. Particle size of powders under hydrothermal conditions. *Crystal Research and Technology: Journal of Experimental and Industrial Crystallography* **2003**, *38*(10), 847-858.

[21] Thanh, N. T., Maclean, N., & Mahiddine, S. Mechanisms of nucleation and growth of nanoparticles in solution. *Chemical reviews* **2014**, *114*(15), 7610-7630.

[22] Welton, T., & Reichardt, C. *Solvents and solvent effects in organic chemistry*. (4th ed) John Wiley & Sons, **2011**, 455-461.

[23] Akerlof, G. Dielectric constants of some organic solvent-water mixtures at various temperatures. *Journal of the American Chemical Society* **1932**, *54*(11), 4125-4139.